SPARC Central Solenoid Cable AC Loss and Quench Detection Studies

National Laboratory **Principal Investigator**	Brookhaven National Laboratory Ramesh Gupta gupta@bnl.gov
Company **Principal Investigator**	Commonwealth Fusion Systems Charlie Sanabria charlie@cfs.energy
Award	INFUSE 2019
Period of Performance	11/1/2019-5/31/2021
Final Report Submission Date	10/21/2021

Note: Report may be posted publicly. Do not include proprietary information.

1 Technical Overview

1.1 Problem Statement

This INFUSE proposal initially set out to test vacuum pressure impregnated, insulated, partially transposed, extruded, and roll-formed (VIPER) cables [1] for quench propagation studies using the Dipole Common Coil (DCC017) operational at the Brookhaven National Laboratory (BNL). The motivation was to understand quench behavior in these cables, which were being considered for use in multiple SPARC systems. After award, this scope was refined to measure AC losses in a variant of VIPER cables, called PIT VIPER, which are being considered for use in the Central Solenoid of SPARC. CFS developed PIT VIPER prior to the start of this INFUSE program with the goal of operating at ramping magnetic fields of up to 4 T/s with manageable AC losses.

The goal of this INFUSE program with BNL was to confirm low AC loss behavior in PIT VIPER cables by applying a ramping magnetic field on both VIPER and PIT VIPER cable samples, and measuring AC losses via calorimetry.

1.2 Test Magnet and Test Facility

The key to this test is BNL's 10 T Nb_3Sn common coil dipole DCC017 [2,3] consisting of a pair of racetrack coils. A unique feature of this magnet is an open or clear space that is large enough to allow insertion and test of a wide range of cable samples and racetrack coils.

BNL also has a number of Dewar and cryogenic facilities to test a variety of magnets. The common coil dipole DCC017 is tested in Dewar 6. In addition, BNL has state-of-the-art instrumentation, including the advanced quench protection system that was utilized in conducting this test. In addition, an acoustic setup developed at the Lawrence Berkley National Laboratory was used in detection and localization of quench. Several Hall probes and temperature sensors were also used.

Figure 1 (left) shows the magnet and Figure 1 (right) shows the opening. The magnet has a unique design with an opening which is 31 mm wide and 335 mm high. The magnet was designed to facilitate a rapid test program where the new cables or coils can be easily inserted and tested in a high field region.

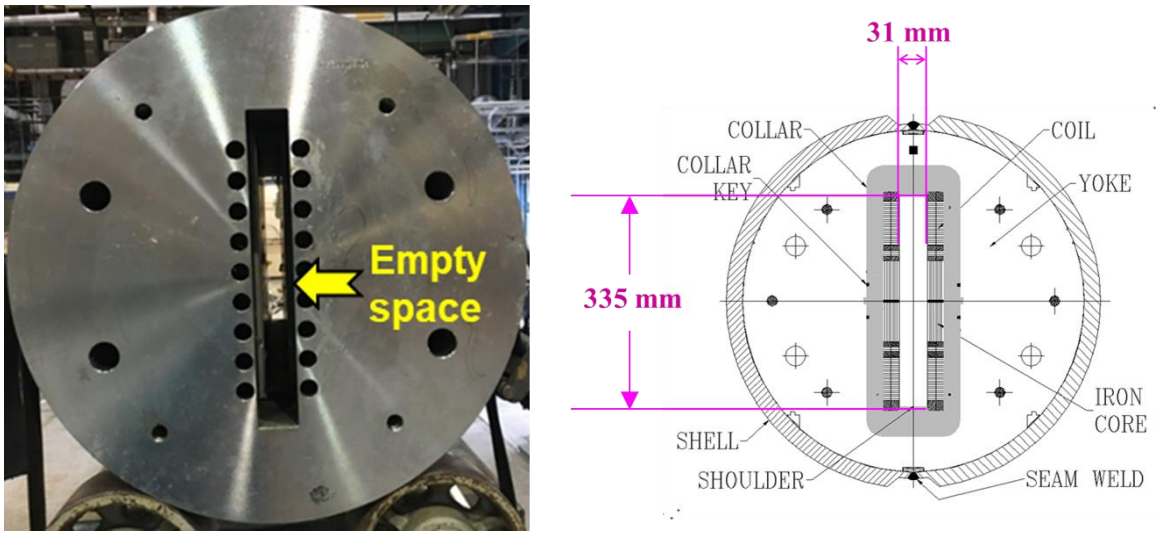

Figure 1 The unique dual-aperture Nb_3Sn dipole magnet at BNL, named DCC017. it has a large opening where coils and cables can be inserted and tested in a dipole field up to 10 T without disassembling the magnet.

Error! Reference source not found. (left) shows the ¾ view of the magnetic model of the dipole DCC017 and **Error! Reference source not found.** (right) shows the vertical cutaway view with the magnitude of the field and field direction superimposed at 10 kA current in Nb_3Sn coils.

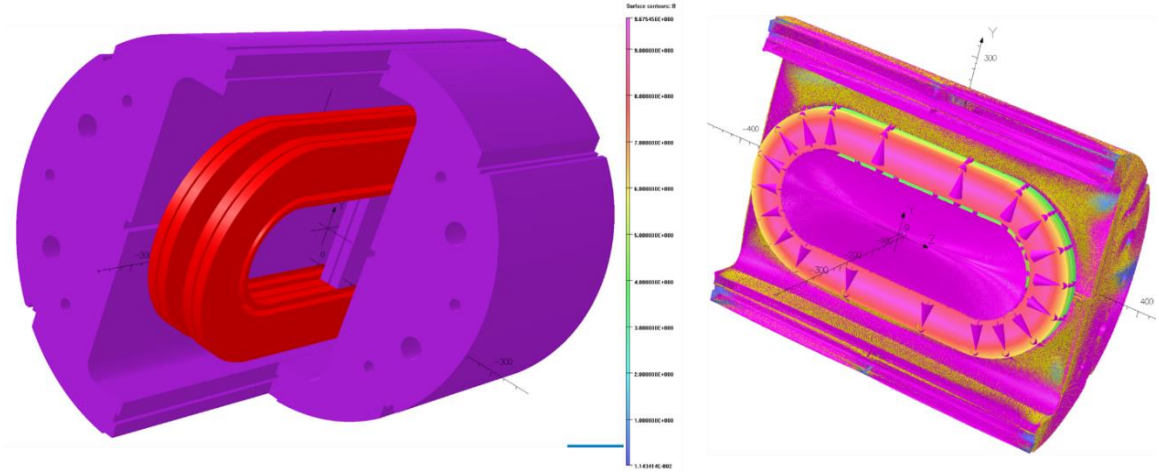

Figure 2 ¾ view of the dipole DCC017 (left) and a vertical cutaway view with the magnitude of the field and field direction superimposed (right) at 10 kA current in Nb_3Sn coils.

Figure 3 shows the fixture that was inserted into DCC017 during a preliminary test made in February 2020. The fixture contained two CFS cable samples as well as two insert HTS test coils for an unrelated high-energy physics (HEP) experiment. All four inserts (two CFS samples and two HTS coils) were tested in the background field and they all experienced a dipole field with the direction of the field as shown in **Error! Reference source not found.**.

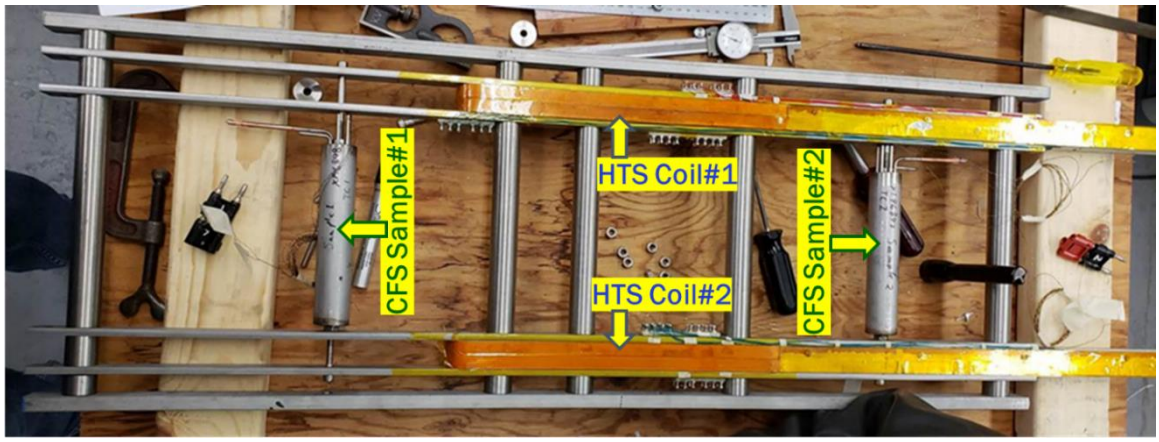

Figure 3 Fixture that was inserted in magnet DCC017 during the test of February 2020. The fixture contained two CFS cable samples and two insert HTS test coils for a HEP experiment. All were tested in the background field.

Figure 4 shows the field in the end region where two CFS cable samples were tested in the background field. The model on the left shows the contour of the magnitude of the field at 10 kA current in DCC017 and line plot on the right shows field as a function of distance on the z-axis.

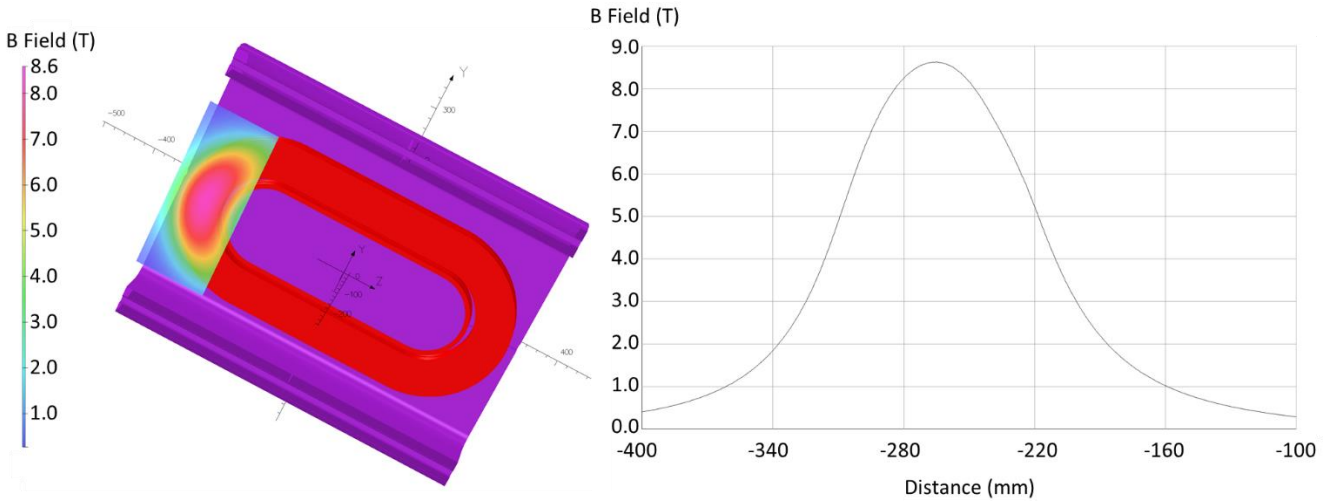

Figure 4 Field in the end region where two CFS cable samples were tested in the background field. The model on the left shows the contour of the magnitude of the field at 10 kA current in DCC017 and the line plot on the right shows field as a function of distance on the z-axis.

Figure 5 shows the line plots of the field at 10 kA (left) as a function of distance on z-axis at center of upper aperture (mirror symmetric for the lower aperture) and (right) as a function of distance on the vertical axis in the upper aperture (mirror symmetric for the lower aperture) where the two sets of CFS samples were tested.

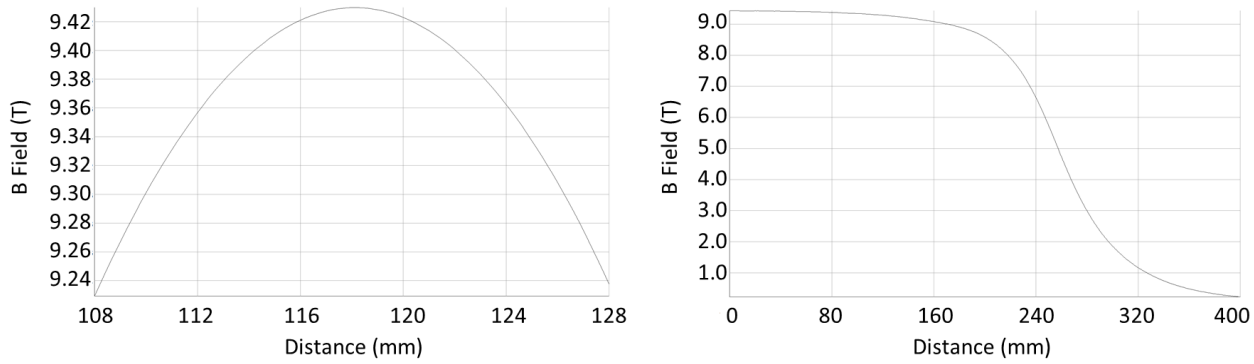

Figure 5 Line plot of the field at 10kA (left) as a function of distance on z-axis at center of upper aperture (mirror symmetric for the lower aperture) and (right) as a function of distance on the vertical axis in the upper aperture (mirror symmetric for the lower aperture) where the two second set of CFS samples were tested.

Figure 6 gives various views of the opening through which the second set of CFS samples in a prefabricated fixture were inserted into DCC017.

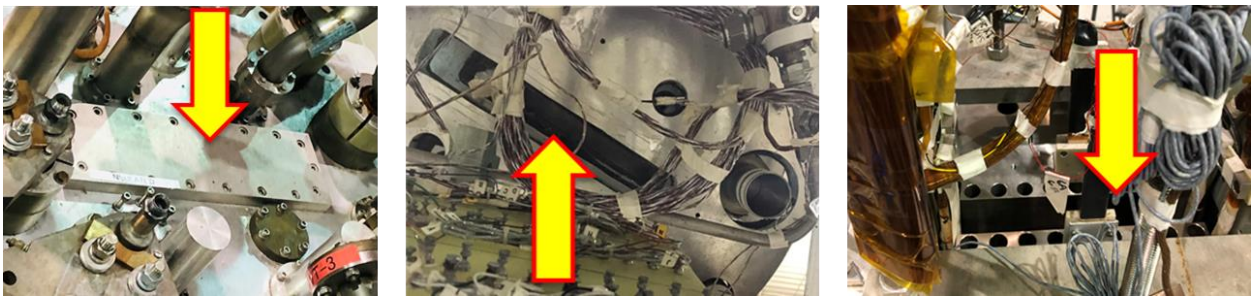

Figure 6 Various views of the wide opening (indicated by the arrow) through which the second set of CFS samples in a prefabricated fixture were inserted into DCC017. The left panel shows the top view of the top-hat with the cover plate, which was removed for inserting CFS fixture. The middle panel shows the view of the top-hat from the bottom showing the opening for the fixture. The right panel shows the opening in the magnet from the top through which the CFS samples were inserted and tested in the background field.

1.3 Work Scope

PIT VIPER and VIPER cable segments were instrumented with Cernox temperature sensors and tested (without current) in the DCC017 Common Coil magnet. The samples (11" long) were subjected to a linearly increasing magnetic field with ramp rates between 0.2 T/s and 0.9 T/s. In addition to the linear ramps, the magnet was quenched intentionally to produce very large magnetic field changes at the magnet's natural L/R decay rate with an exponential time constant of roughly 60 ms. In each case, the temperature rise of these thermally insulated samples was measured and the enthalpy calculated.

The magnet operates in a liquid helium bath (4.2 K), which makes thermal insulation and instrumentation very challenging. The samples were fully encased in stainless steel vacuum vessels and the instrumentation was routed (in vacuum) to room temperature where standard vacuum D-sub (DB-25) connector feedthroughs were used to extract the signals, as shown in Figure 7. Figure 8 shows the vacuum vessel and G-10 support dimensions, and Figure 9 shows the instrumentation used. Three Cernox sensors per sample were used, and additional Cernox sensors were located on the G-10 holders and a tape stack (control samples). A Hall probe was placed at each box center.

Additional samples were used to test the ability of acoustic and fiber-optic systems to measure temperature rise. These samples are named QA and QF respectively (Figure 9).

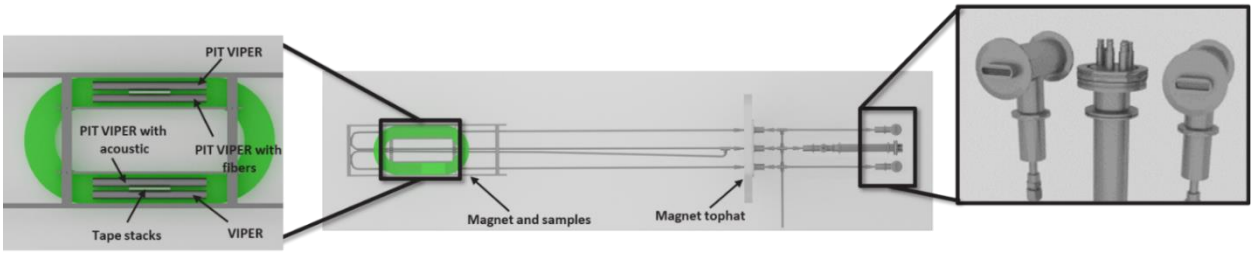

Figure 7 – Experimental setup and feedthrough instrumentation. Left: closeup at the sample position with respect to the coils. Middle: Rig overview showing the sample region, the top hat, and the signal extraction feedthroughs. Right: Vacuum D sub (DB-25) connector feedthroughs and fiberoptic feedthroughs used to extract the signals.

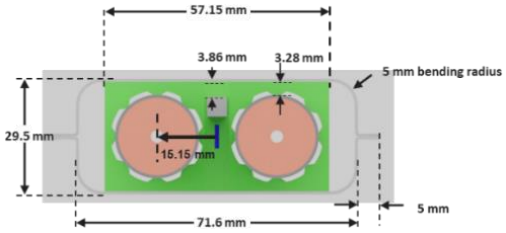

Figure 8 – Dimensions of the sample boxes.

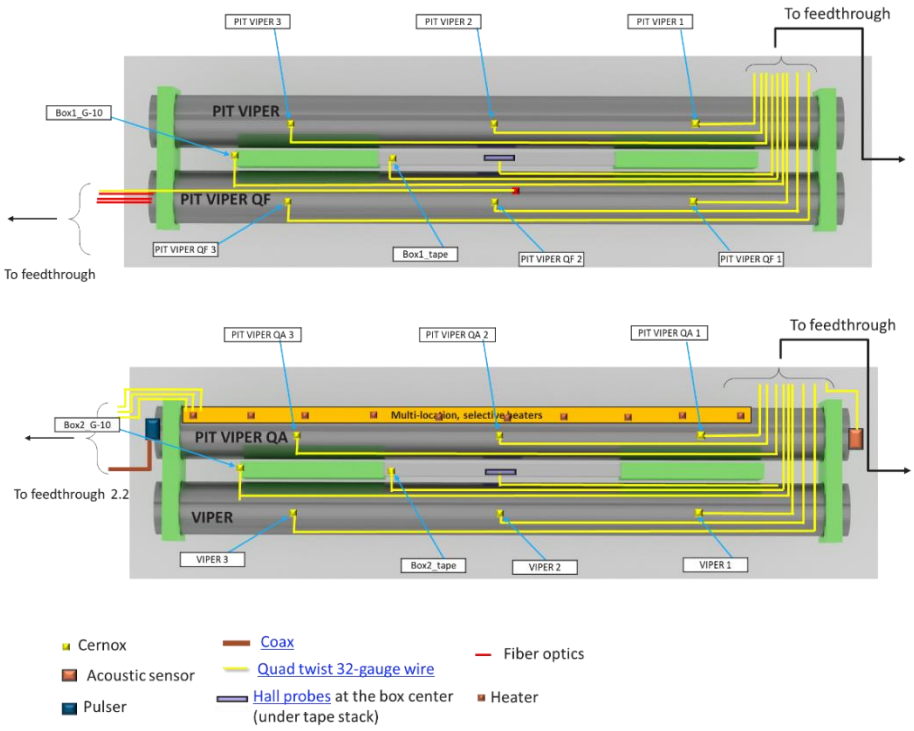

Figure 9 – Overview of the sample instrumentation sketched over the samples to illustrate their relative positioning. Three Cernox sensors per sample were used, and additional Cernox sensors were located on the G-10 holders and a tape stack (control samples). A Hall probe was placed at each box center.

1.4 Sample manufacture and installation.

The samples shown schematically in Figure 9 were manufactured and assembled in-house at CFS, as shown in Figures 10-12.

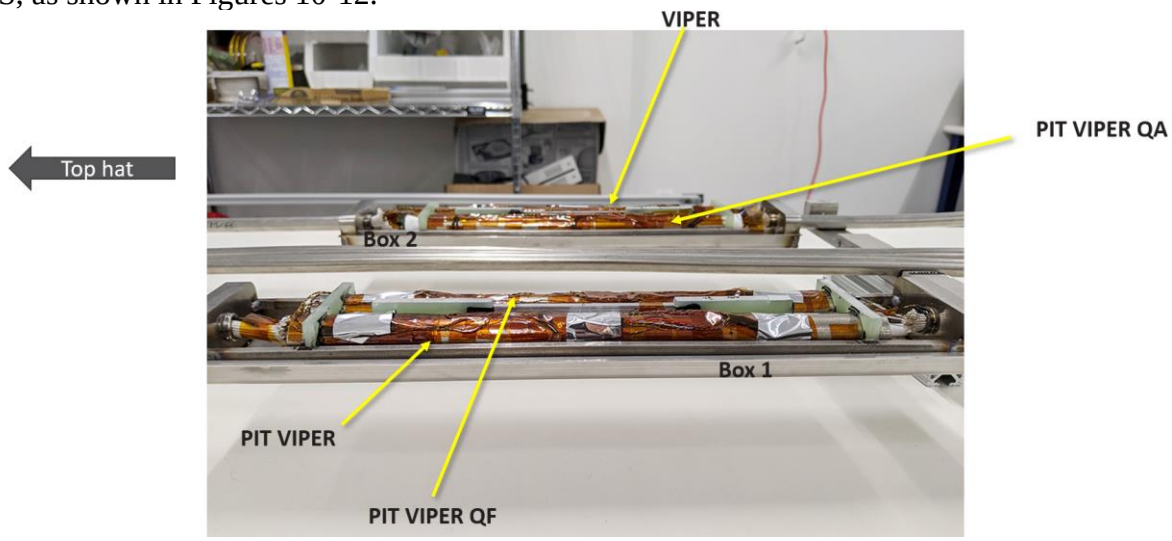

Figure 10 – Sample assembly at CFS. Additional samples were used to investigate test the ability of acoustic and fiber-optic systems to measure the temperature rise detection capabilities using acoustic and fiber optic systems for the samples. These samples are named QA and QF respectively.

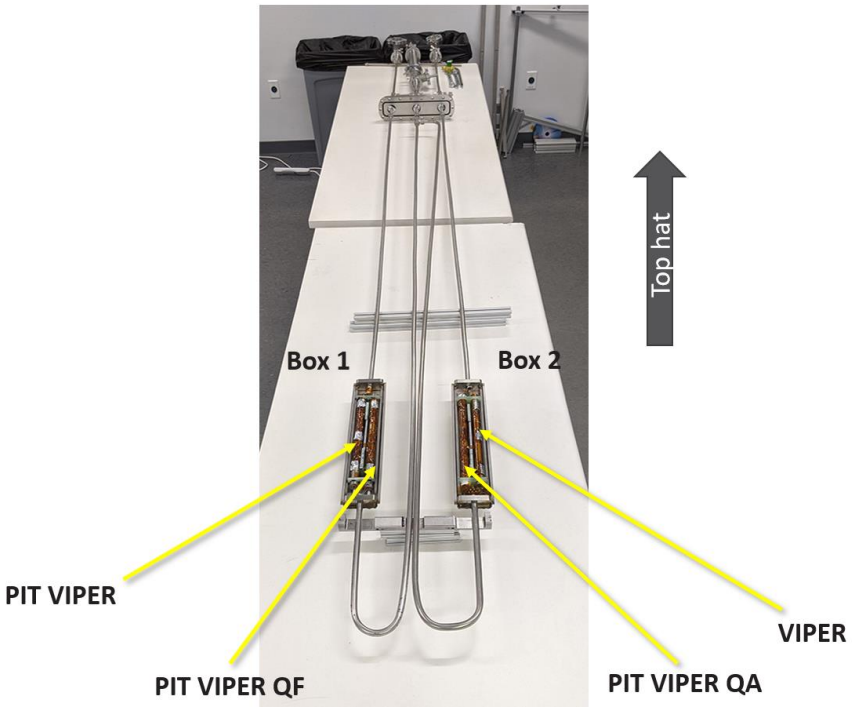

Figure 11 – Full samples shown before enclosure.

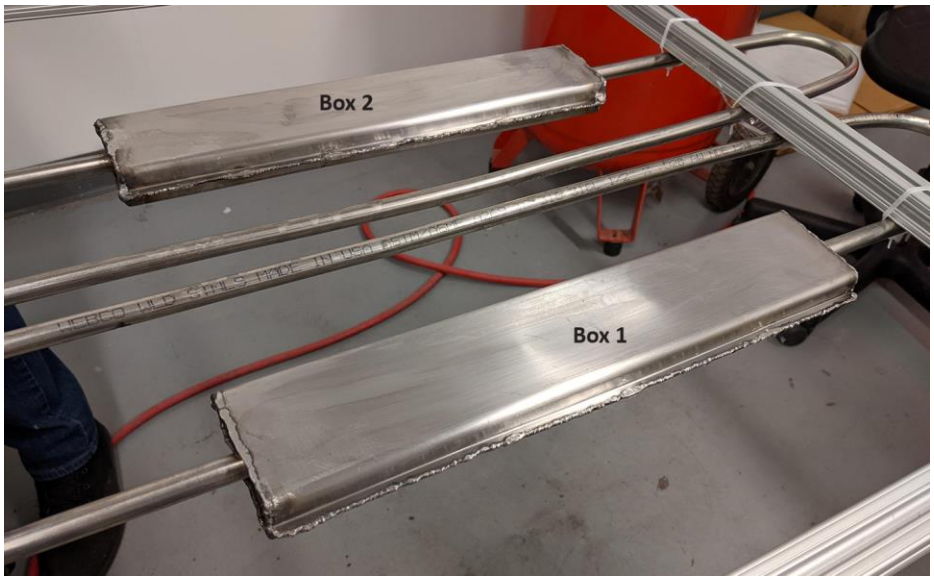

Figure 12 – Welded sample boxes ready for transport.

Upon arrival at BNL, the standard suite of fit and leak checks was performed. It was discovered that tolerances were tighter than expected and the sample boxes needed to be ground and rewelded to fit into the bore space. After grinding and rewelding to seal any gaps, leak checks were performed again and the sample was cleared for insertion into the Common Coil (Figure 13).

Figure 13 – Sample ready for installation into magnet bore.

1.5 Results

The data collected during the test included current, temperature, and magnetic field. The current of the Common Coil was measured using a zero-flux DC current transformer. The cable sample temperature was measured using Cernox sensors. And the magnetic field was measured using Hall Probes. The "nominal" magnetic fields of the various runs are shown in Table 1 and the traces in Figure 14. These nominal field values were approximated by the interpolation of a known field at a known current (10.2 T at 10.8 kA) and the zero-field, zero-current state of the common coil.

These results indicated that higher ramp rates could be obtained if the field was decreasing, and that a maximum "nominal" dB/dt of -0.94 T/s was achieved from a peak field of 5.68 T without quenching the magnet.

Table 1 – Peak field and target dB/dt values for the runs analyzed

	Description	Peak Field	Target dB/dt
Run 1	Ramp	7.57	0.28
Run 2	Ramp	2.76	0.38
Run 3	Ramp	7.57	0.28
Run 4	Ramp	7.57	-0.28
Run 5	Ramp	2.38	0.38
Run 6	Ramp	7.57	0.19
Run 7	Quench	7.57	≈ -30 T (see Figure 14)
Run 8	Ramp	5.68	0.24
Run 9	Quench	5.68	See Figure 14
Run 10	Ramp	2.37	0.56
Run 11	Ramp	5.68	0.19
Run 12	Quench	5.68	≈ -9 T (see Figure 14)
Run 13	Ramp	3.79	-0.94
Run 14	Ramp	5.68	-0.94
Run 15	Ramp & quench	7.57	≈ -25 T (see Figure 14)

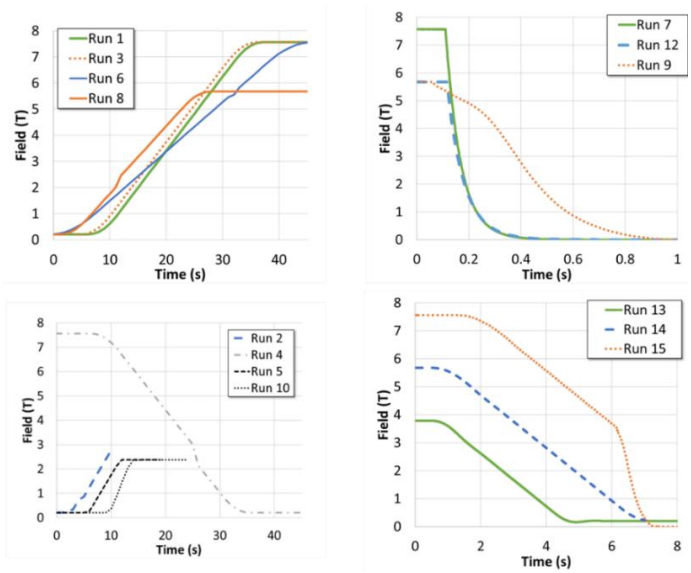

Figure 14 – Nominal field evolution of the various runs analyzed.

The Hall probe on Box 1 became unresponsive prior to testing and the Hall probe on Box 2 became unresponsive during testing. Fortunately, the Hall probe on Box 2 was operating up until Runs 3 and 4, allowing us to measure the highest magnetic field used during testing. A field of 7 T was measured when the approximated nominal field was 7.57 T. This difference is shown in Figure 15 below, indicating that the measured field can be around 5% lower than the nominal field. No further field data was measured directly after the hall probes failed.

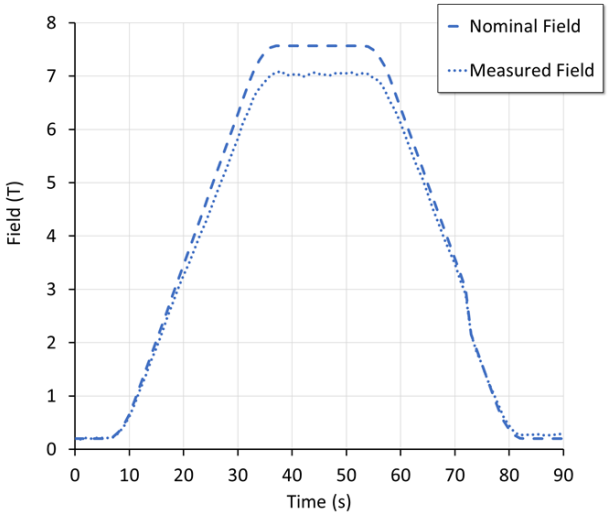

Figure 15 – Nominal field and measured field at the center of the box for Runs 3 and 4 (ramp up and ramp down respectively).

Using the temperature changes, ΔT, and the sample's mass and instantaneous heat capacity, the instantaneous heating per meter, q, and the total joules generated, Q, were calculated using equations 1 and 2 below:

$$q = \frac{m \cdot C_p(T) \cdot \Delta T}{sample\ length} \qquad (1)$$

$$Q = \sum_{i=0}^{n} m \cdot C_p(T) \cdot \Delta T_i \qquad (2)$$

Figure 16 shows examples of the ΔT, q, and Q for a characteristic run. The peak heating and total heat for one of the runs are shown in Table 2 below. The dB/dt of the run is not shown to protect CFS' IP.

Table 2 – example calculations of peak heating and total heat measured on one of the runs. The dB/dt of the run is not shown to protect CFS' IP.

Sample	Peak Heating (W/m)	Total heat (J)
PIT VIPER	1.72	1.58
VIPER	72.01	51.94

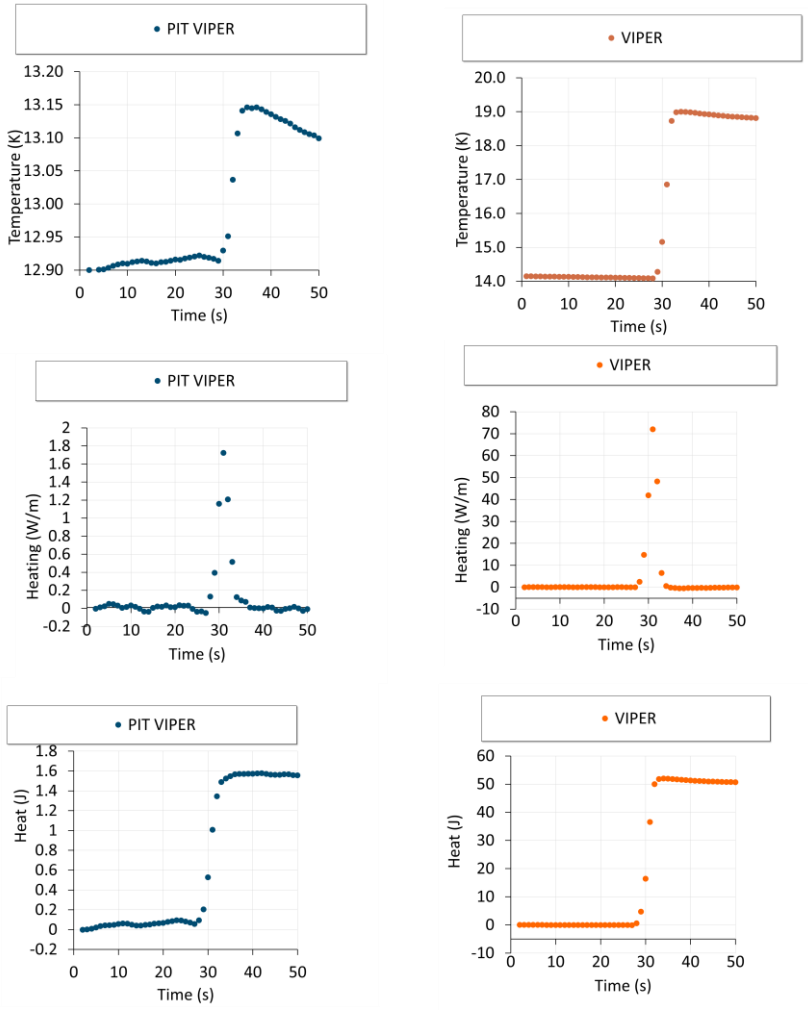

Figure 16 – Heating and accumulated heat evolution for one of the runs. The dB/dt of the run is not shown to protect CFS' IP.

As observed in Figure 16 and Table 2, the heating observed was more than 40 times lower for PIT VIPER than VIPER. The other fourteen runs are not shown in this report, but they further confirm the AC loss tolerance of PIT VIPER cables.

2 Impact

2.1 Use of Project Results

The experimentally obtained AC loss values for PIT VIPER helps CFS refine the finite element models used to calculate heating in the SPARC Central Solenoid, and improve magnet design. The results obtained show very promising performance for PIT VIPER cables and allows CFS to move forward with the Central Solenoid Model Coil (CSMC) project sponsored under an ARPA-E grant. We are projected to perform similar tests in the near future for PIT VIPER joint AC loss measurements as well as quench propagation studies to further understand the capabilities of PIT VIPER and the limitations for fast ramping HTS magnets.

Figure 17 shows the intersections of CFS' 2019 INFUSE programs with the SPARC timeline: this project (bottom right) provided data for SPARC's CS Conceptual Design Review (CDR) and Preliminary Design Review (PDR).

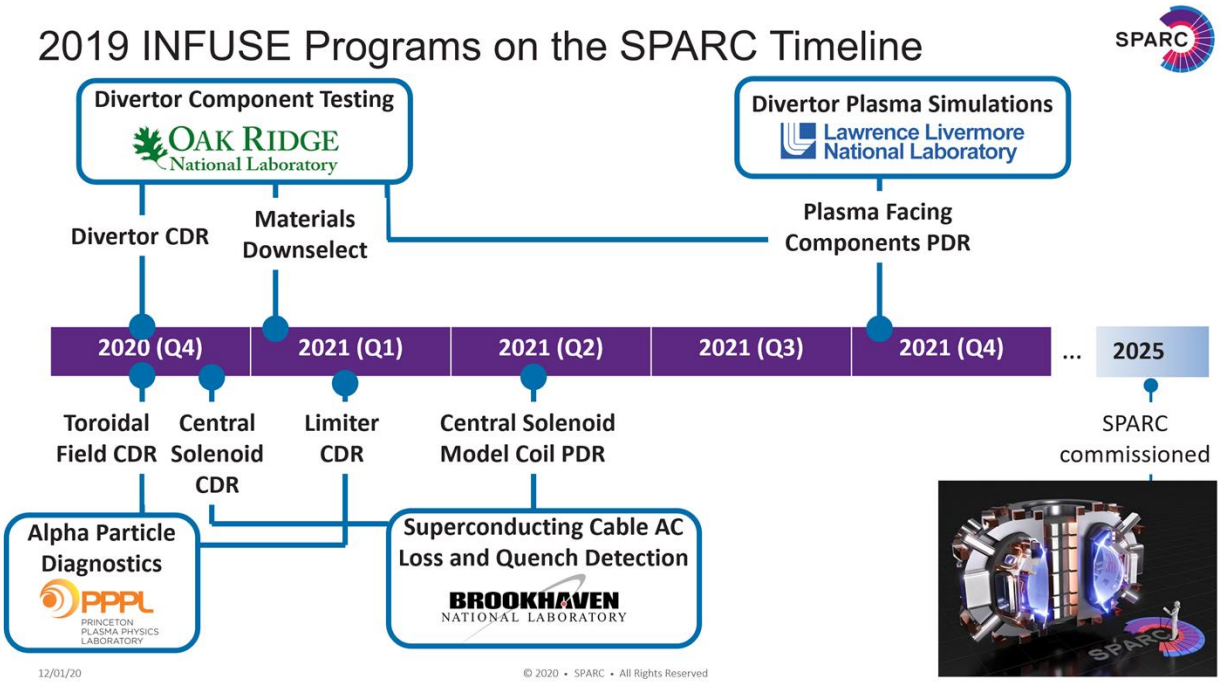

Figure 17 Intersections of CFS' 2019 INFUSE programs with the SPARC timeline.

2.2 Fusion Energy Impact

A fast ramping HTS Central Solenoid makes a pulsed tokamak a feasible and economical power plant. In such a machine, plasma current is driven and maintained inductively rather than with an external current drive. Relative to a steady-state tokamak, a pulsed tokamak is expected to produce

power at approximately half the cost per Watt, due to reduced recirculating power and the elimination of any external current drive. Therefore, the demonstration of a fast-ramping HTS coil like the SPARC CSMC—under an ARPA-E grant and for which this INFUSE proposal was essential—enables a new, lower-risk path to lower-cost commercial fusion energy. We calculate that a pulsed tokamak using HTS for each of its three magnet systems (Toroidal, Poloidal and Central) will produce power below $4/W and will have an OCC < $1B.

In addition to making SPARC more economically feasible, an HTS CS also makes SPARC a significantly more complete risk retirement of a pulsed tokamak commercial device, and places it more directly on the commercialization pathway. Solving the unique engineering challenges associated with a fast-ramping CS would enable SPARC's Poloidal Field coils to be made from HTS as well.

2.3 Intellectual Property, Publications and Conferences

(None projected)

3 References

1. Hartwig, Z. S. et al. VIPER: an industrially scalable high-current high-temperature superconductor cable. Supercond. Sci. Technol. **33**, 11LT01 (2020).
2. R. Gupta, et al., "React & Wind Nb_3Sn Common Coil Dipole," IEEE Transactions on Applied Superconductivity, Vol. 17, No. 2, (2007), pp 1130-1135.
3. R. Gupta et al., "New Approach and Test Facility for High-Field Accelerator Magnets R&D," in IEEE Transactions on Applied Superconductivity, vol. 30, no. 4, pp. 1-6, June 2020, Art no. 4000106, doi: 10.1109/TASC.2019.2961064.